JACS
JOURNAL OF THE AMERICAN CHEMICAL SOCIETY
Article
pubs.acs.org/JACS

Structure and Thermodynamics of N^6-Methyladenosine in RNA: A Spring-Loaded Base Modification

Caroline Roost,[†] Stephen R. Lynch,[†] Pedro J. Batista,[‡] Kun Qu,[‡] Howard Y. Chang,*[,‡] and Eric T. Kool*[,†]

[†]Department of Chemistry, [‡]Howard Hughes Medical Institute and Program in Epithelial Biology, Stanford University, Stanford, California 94305, United States

Supporting Information

ABSTRACT: N^6-Methyladenosine (m^{6}A) modification is hypothesized to control processes such as RNA degradation, localization, and splicing. However, the molecular mechanisms by which this occurs are unclear. Here, we measured structures of an RNA duplex containing m^{6}A in the GGACU consensus, along with an unmodified RNA control, by 2D NMR. The data show that m^{6}A–U pairing in the double-stranded context is accompanied by the methylamino group rotating from its energetically preferred *syn* geometry on the Watson–Crick face to the higher-energy *anti* conformation, positioning the methyl group in the major groove. Thermodynamic measurements of m^{6}A in duplexes reveal that it is destabilizing by 0.5–1.7 kcal/mol. In contrast, we show that m^{6}A in unpaired positions base stacks considerably more strongly than the unmodified base, adding substantial stabilization in single-stranded locations. Transcriptome-wide nuclease mapping of methylated RNA secondary structure from human cells reveals a structural transition at methylated adenosines, with a tendency to single-stranded structure adjacent to the modified base.

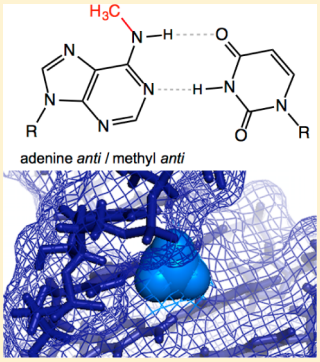

INTRODUCTION

Post-transcriptionally modified bases in RNA are numerous and important to cellular function. The most common internal RNA modification in eukaryotes is adenine N^6-methylation (Figure 1),[1] which occurs, on average, at three sites per mRNA and is found on long noncoding RNAs as well.[2,3] Numbers of substitutions per RNA vary from one to as many as 11 or more. Although the effect of methylation in codons on translation has yet to be determined, methylation loci occur most commonly in 3′ UTRs and near splice sites, suggesting a more common role in signaling and control rather than directly in protein coding. In this light, methylation has been shown to shorten the average lifetime of RNAs and to influence their subcellular localization.[4] Significantly, the effect of this substitution on RNA structure and folding is not known for any of the thousands of RNAs that contain the modification.

Although this RNA modification has been studied for decades, the biology and biochemistry of m^{6}A methylation and demethylation is emerging rapidly in recent years. A methylation complex including enzyme METTL3 has been identified and shown to perform adenine methylation in eukaryotic cells,[5,6] and FTO and AlkBH5 are two oxidative proteins that have been demonstrated to accomplish demethylation *in vitro*.[7,8] The functions of these latter enzymes are associated with important physiological pathways including metabolism and fertility.[8−10] Moreover, polymorphic variations in the FTO gene have been linked to breast and endometrial cancer risk.[11−13]

Because both methylating and demethylating factors have been identified, m^{6}A modification is hypothesized to act as a biological switch of RNA activity.[14] However, the molecular mechanism by which methylation status affects biological pathways is as yet unclear. Current hypotheses have focused mainly on the possibility that proteins specifically recognize and bind m^{6}A,[15] marking the modification for further downstream events.

Here, we consider another possible mechanism by which N6 methylation might affect biological activities of RNAs: by altering their stability and conformation. The 6-methyl group on an adenine base alone in solution is known to exist in two conformations, with *syn* being energetically favored by ca. 1.5 kcal/mol over *anti* (Figure 1).[16] Consistent with this, in the solid state it resides in *syn* orientation.[17] The structure of the modified base in paired RNA is unknown; in single strands, it likely adopts the favored *syn* conformation,[18] but in pairing positions, this is not clear. Indeed, simple inspection of base pairing models (Figure 1C) suggests at least three possible structures for m^{6}A paired within duplexes. The question of which of these is formed could well-affect pairing geometry and stability of folded RNAs and ultimately the biology of this modification.

To study this question, here we have carried out biophysical and structural studies of discrete m^{6}A residues in short RNAs. We report that single m^{6}A modifications are destabilizing to RNA duplexes that contain them, but, in contrast, they are strongly stabilizing in unpaired positions adjacent to duplexes. We further show that the N6 methylamino group must distort to a high-energy conformation, rotating the methyl group into the major groove, in order to be accommodated into a locally

Received: December 23, 2014
Published: January 22, 2015

DOI: 10.1021/ja513080v
J. Am. Chem. Soc. 2015, 137, 2107−2115

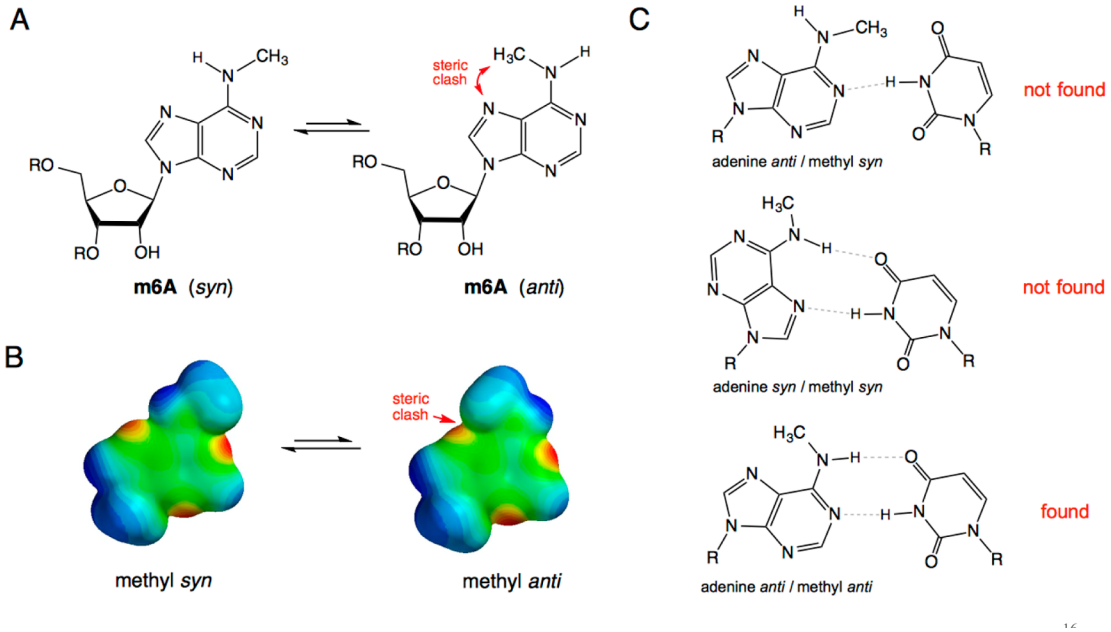

Figure 1. Structures and conformations of m^{6}A in RNA. (A) *Syn* methyl orientation is favored over *anti* when the base is unpaired[16] as a result of a steric clash between the methyl group and N7. (B) Space-filling models of m^{6}A in *syn* and *anti* conformations (N9 substituent is methyl). (C) Multiple pairing configurations are possible for m^{6}A paired opposite U; these configurations vary on whether the adenine base and the methylamino group are *syn* or *anti*. The current work confirms the third (*anti*/*anti*) structure in an RNA duplex; the methyl group is spring-loaded into the high-energy *anti* conformation, trapped there by pairing with U and surrounding duplex structure.

paired helix. This suggests that enzymatic methylation in paired regions of RNA and, conversely, demethylation in unpaired regions could destabilize existing structure, possibly triggering larger conformation changes in the RNA and altering its susceptibility to degradation. Preliminary data mapping the structure of methylated sites in cellular RNAs reveals the presence of a structural transition near the methylated adenosine, consistent with the notion that m^{6}A is preferentially situated at the transition between unpaired and duplex structure.

EXPERIMENTAL SECTION

RNA Synthesis. RNA oligonucleotides were synthesized using standard β-cyanoethyl phosphoramidite chemistry and 2′-*O*-TBDMS-protected ribonucleosides. The m^{6}A phosphoramidite derivative was synthesized according to literature procedures.[19] RNA oligonucleotides were purified by denaturing polyacrylamide gel electrophoresis and characterized by MALDI-MS. See Supporting Information for details and data.

Thermal Denaturation Experiments. Solutions for the thermal melting experiments contained a 1:1 ratio of two complementary strands in 1−5 μM total RNA concentration (C_t). Self-complementary cases were measured in 2−14 μM concentrations. The oligoribonucleotides were measured in 10 mM sodium phosphate buffer, pH 7.0, with 1 M NaCl. Prior to the measurements, solutions were heated at 90 °C and then slowly cooled to 10 °C to ensure a complete annealing of the strands. Absorbance at 260 nm was monitored while temperature was raised at a rate of 1 °C/min from 10 to 90 °C. Thermodynamics were derived via curve-fitting with the standard two-state model and by van't Hoff fitting of data from varied concentrations. See Supporting Information for details and data.

NMR Methods. NMR experiments were acquired on a Varian Inova 600 MHz spectrometer with a z-gradient triple resonance HCN probe or a Varian Inova 500 MHz spectrometer with a z-gradient H{X} probe. ^{1}H and ^{13}C chemical shifts were referenced indirectly to tetramethylsilane (TMS); ^{31}P shifts were referenced indirectly referenced to phosphoric acid. The exchangeable ^{1}H resonances of the duplexes were assigned using through-space homonuclear SS-NOESY experiments at 15 °C with different mixing times (100 or 250 ms) on a sample in 90% H_20/10% D_2O. The nonexchangeable ^{1}H resonances of the RNA were assigned with a combination of homonuclear NOESY experiments at varied mixing times (75, 150, and 300 ms), DQF-COSY, homonuclear TOCSY with 80 ms mixing time, ^{1}H/^{13}C HSQC, and ^{1}H/^{31}P heteronuclear COSY acquired at 25 °C on a sample dissolved in 99.996% D_2O. See Supporting Information for details.

Structure Calculations. Structures were calculated using restrained molecular dynamics followed by energy minimization using the program XPLOR-NIH, version 2.35, with a force field consisting of bond lengths, bond angles, improper angles, repulsive van der Waals potentials, and experimental distance and dihedral constraints in the absence of electrostatics. Random starting structures were created by randomizing torsion angles for the calculation. See Supporting Information for details. Structures of the averaged duplexes have been deposited with the PDB (2MVY and 2MVS).

RNA Isolation and m^{6}A Enrichment. GM12878 cells were cultured as described.[20] Cells were collected at a confluence of 6×10^5 cells per milliliter, and RNA was extracted with TRIzol according to the manufacturer's protocol. m^{6}A immunoprecipitation and library construction were done as described by Batista et al.[21] PolyA RNA selection was performed using MicroPoly(A) Purist (Life Technologies) according to the manufacturer's protocol. The PolyA+ RNA was fragmented to ∼100 nucleotide fragments by incubation in a zinc buffer (10 mM $ZnCl_2$, 10 mM Tris-HCl, pH 7.0) for 2 min followed by ethanol precipitation. Methylated RNA was selected as described[22] using anti-m^{6}A polyclonal antibody (Synaptic Systems). The immunoprecipitated RNA and an equivalent amount of input RNA were used for library generation with the dUTP protocol, as described,[23] except that libraries were size selected by gel purification after ligation and after PCR amplification. Libraries were sequenced using an Illumina HiSeq at the Stanford Center for Genomics and Personalized Medicine. For all libraries, single-end RNA-Seq reads were mapped to the human genome (hg19 assembly) using TopHat (version 1.1.3).[24] Only uniquely mapped reads were subjected to downstream analyses. A nonredundant hg19 transcriptome was assembled from UCSC RefSeq genes and UCSC genes. The search for enriched peaks was performed by scanning each gene using 100

DOI: 10.1021/ja513080v
J. Am. Chem. Soc. 2015, 137, 2107−2115

nucleotide sliding windows and calculating an enrichment score for each sliding window.[2] To determine high-confidence sites, we intersected the peaks with m^{6}A sites from ref 16. See Supporting Information for details.

PARS Mapping of RNAs. Nuclease V1 and S1 were used to map secondary structure of RNAs as described.[20] PARS scores for the neighborhood of RRACH motifs were obtained from ref 20.

RESULTS

Adenine N6 Methylation Is Destabilizing in Base-Paired Regions of RNA. To evaluate the effect of m^{6}A substitution on the stability of paired regions of RNA, we synthesized 8-mer RNA strands containing single m^{6}A substitutions in two different sequence contexts as well as complementary RNAs for each. We also prepared a 10-mer self-complementary RNAs containing two sites of substitution, and these were used for thermodynamic and structural studies (see below). Sequences are shown in Table 1; one single-substitution sequence and the double-substitution sequence correspond to common methylation consensus sequences (GGAGU and CGACU),[2,3,5] and one single-substitution sequence does not. We measured thermodynamics of duplex formation by UV-monitored thermal denaturation and obtained free energies from curve fitting and from van't Hoff measurements. Primary data are given in the Supporting Information (Figures S1 and S2). All duplexes exhibited two-state behavior, as judged by good agreement of the two-state fitting model with the van't Hoff data.

Table 1. Thermal Denaturation Data for Base Pairing of m^{6}A Compared with A

	Duplex	T_m (°C)*	$\Delta G°_{37}$ fit (kcal/ mol)**	$\Delta G°_{37}$ vH (kcal/ mol)†	$\Delta G°_{37}$ avg (kcal/ mol)‡
1	5′UACGACUG AUGCUGAC 5′	47.4 ± 0.1	-10.7 ± 0.1	-10.9 ± 0.2	-10.8 ± 0.2
2	5′UACGACUG AUGCAGAC 5′	23.1 ± 0.4	-6.1 ± 0.1	-6.0 ± 0.2	-6.1 ± 0.2
3	5′UACGACUG AUGCGGAC 5′	29.9 ± 0.1	-7.3 ± 0.1	-6.9 ± 0.2	-7.1 ± 0.2
4	5′UACGACUG AUGCCGAC 5′	33.2 ± 0.3	-8.0 ± 0.1	-8.5 ± 0.1	-8.3 ± 0.1
5	5′UACGÂCUG AUGCUGAC 5′	43.7 ± 0.2	-10.2 ± 0.1	-10.5 ± 0.1	-10.4±0.1
6	5′UACGÂCUG AUGCAGAC 5′	24.3 ± 0.1	-6.3 ± 0.1	-5.3 ± 0.5	-5.8 ± 0.5
7	5′UACGÂCUG AUGCGGAC 5′	27.3 ± 0.1	-6.8 ± 0.1	-7.0 ± 0.2	-6.9 ± 0.2
8	5′UACGÂCUG AUGCCGAC 5′	28.3 ± 0.2	-7.0 ± 0.1	-7.5 ± 0.1	-7.3 ± 0.1
9	5′CGAUAGGU GCUAUCCA 5′	49.9 ± 0.2	-11.5 ± 0.1	-11.3 ± 0.2	-11.4 ± 0.2
10	5′CGAUÂGGU GCUAUCCA 5′	44.2 ± 0.1	-10.2 ± 0.1	-9.2 ± 0.1	-9.7 ± 0.1
11	5′GGACUAGUCC CCUGAUCAGG 5′	70.6 ± 0.1	-16.4 ± 0.1	-14.3 ± 0.2	-15.4 ± 0.2
12	5′GGÂCUAGUCC CCUGAUCÂGG 5′	64.4 ± 0.4	-15.0 ± 0.2	-13.5 ± 0.2	-14.2 ± 0.2

*Conditions: 100 mM NaCl, 10 mM $MgCl_2$, 10 mM Na-PIPES (pH 7.0), [5 μM] duplex. **Averaged free energies derived from two-state curve fits. †Free energies derived from van't Hoff linear plots. ‡Average of free energy from curve fits and van't Hoff plots.

The experiments show that N6 methylation is consistently destabilizing to RNA duplexes when substituted opposite a complementary U within the helix. In one single-substitution context (Table 1, entries 1 and 5), the amount of destabilization is relatively small (0.5 kcal/mol (37 °C)), whereas in the second context (entries 9 and 10), the cost is considerably larger (1.7 kcal/mol). For the double-substitution context, the destabilization amounts to 0.6 kcal/mol per methyl. These values are consistent with an early study of polymer RNAs, which suggested destabilization of 0.5−1.0 kcal/mol,[18] and with a report of Kierzek,[25] which identified a destabilization of ∼1.1 kcal per methyl in doubly substituted RNAs. The current experiments, the first to test the effects of single methyl groups and multiple sequence contexts, establish that there is a strong dependence of stability on context.

We are aware of no prior reports measuring pairing selectivity of N^6-methylA in RNA; therefore, we carried out experiments to evaluate this parameter. Despite the destabilization caused by m^{6}A, our studies pairing it opposite varied bases show that m^{6}A retains selectivity for its Watson−Crick complement U (Table 1, entries 6−8 compared with entries 2−4 in the unmethylated case). The average pairing selectivity of m^{6}A is similar to that of A; the chief differences are the greater selectivity of m^{6}A against pairing with C and the slightly lower selectivity against pairing with A or G. Taken together, the pairing data suggest that the pairing destabilization, more than altered pairing selectivity, is likely to have the largest influence on structure.

Adenine N6 Methylation Stabilizes Base Stacking at Helix Ends. Since stability of folded nucleic acids depends heavily on base stacking,[26] we measured the effect of N6 methyation on the stacking of adenine in unpaired (dangling-end) contexts at the 5′ and 3′ ends of a hexamer core duplex. The data and sequences are given in Table 2. As is well-established,[26] adenine stacks relatively strongly on adjacent duplexes, especially at their 3′ end; here, we find a stabilization of 1.5 kcal/mol for addition of two 3′ dangling (unmodified) adenosine residues (0.75 kcal/mol per adenosine) and a smaller stacking stabilization of 0.26 kcal per adenosine at the 5′ end in the same context (compare entries 2 and 4 to entry 1), consistent with prior studies.[26] Significantly, we find that methylation affects stacking of adenine strongly: m^{6}A stacks 0.42 kcal/mol per methyl more strongly than A at the 3′ end and 0.58 kcal more strongly at the 5′ end (entries 3 and 5). Adenine is the strongest stacking of the four RNA bases,[26] and we find here that addition of a methyl group enhances stacking

Table 2. Thermal Denaturation Data for m^{6}A End Stacking in Self-Complementary Duplexes

	Duplex	T_m (°C)*	$\Delta G°_{37}$ fit (kcal/ mol)**	$\Delta G°_{37}$ vH (kcal/ mol)†	$\Delta G°_{37}$ avg (kcal/ mol)‡
1	5′CGCGCG GCGCGC 5′	53.3 ± 0.2	-10.2 ± 0.1	-11.6 ± 0.1	-10.9 ± 0.1
2	5′ CGCGCGA AGCGCGC 5′	61.4 ± 0.1	-12.1 ± 0.1	-12.7 ± 0.1	-12.4 ± 0.1
3	5′ CGCGCG^{m}A ^{m}AGCGCGC 5′	62.7 ± 0.4	-12.4 ± 0.1	-14.1 ± 0.2	-13.2 ± 0.2
4	5′ ACGCGCG GCGCGCA 5′	56.3 ± 0.2	-10.8 ± 0.2	-12.0 ± 0.2	-11.4 ± 0.2
5	5′^{m}ACGCGCG GCGCGC^{m}A 5′	59.7 ± 0.3	-11.6 ± 0.1	-13.5 ± 0.2	-12.6 ± 0.2

*Conditions: 100 mM NaCl, 10 mM $MgCl_2$, 10 mM Na-PIPES (pH 7.0), [5 μM] duplex. **Averaged free energies derived from two-state curve fits. †Free energies derived from van't Hoff linear plots. ‡Average of free energy from curve fits and van't Hoff plots.

DOI: 10.1021/ja513080v
J. Am. Chem. Soc. 2015, 137, 2107−2115

by as much, on average, as the entire nucleobase adenine does alone. This favorable stacking likely arises from hydrophobic shielding of the methyl group against neighboring bases.[27] Thus, it is clear that in these contexts m^{6}A modification of an unpaired adenine substantially increases the stability of nearby helices. Importantly, this is the opposite effect that the N6 modification has within duplexes, and it is of similar magnitude.

Structures of Methylated and Unmethylated RNAs Reveal a Conformational Switch in m^{6}A upon Pairing. To study the structural origins of destabilization by m^{6}A when paired, next we studied the structures of a duplex RNA containing m^{6}A residues (denoted MA) and of a control RNA lacking the modification (AD) in solution. The self-complementary sequences are shown in Table 1, entries 9 and 10, and contain the common GGACU methylation consensus. The downfield portion of the 1D ^{1}H NMR in H_2O spectra is shown in Figure 2. The five resonances observed

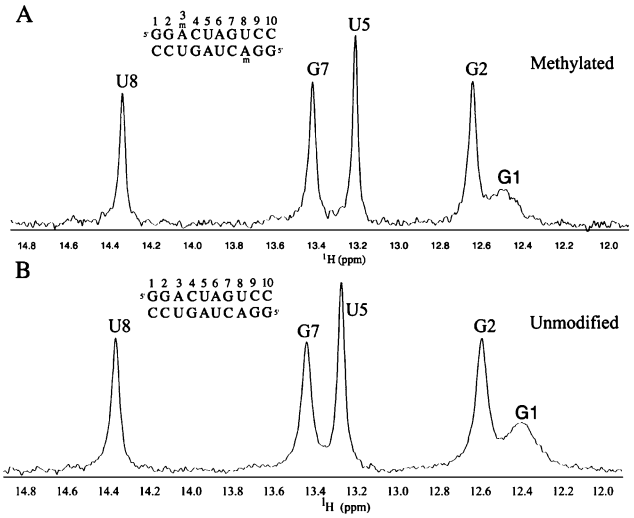

Figure 2. Proton NMR spectra of RNA duplexes containing GGACU methylation motif, confirming fully paired structure. (A) 1D proton spectrum of methylated duplex; (B) spectrum of unmethylated duplex for comparison. Downfield regions of the 1D ^{1}H NMR spectra are shown; they were acquired in 90% H_2O/10% D_2O at 15 °C with 11 solvent suppression and show evidence of 10 H-bonded base pairs (5 symmetrically unique) for methylated duplex MA (A) and unmodified AD (B).

in both spectra are the imino resonances of uridine and guanosine, confirming that both duplexes are fully base-paired (note that each duplex has five symmetrically unique pairs). The imino resonances are shifted downfield as a result of hydrogen bonding and are sharp, indicating a slow exchange rate with water. The only broadened resonance corresponds to G1 in the end base pair, which is more exposed to solvent. The chemical shift for the NH of U8, opposite m^{6}A3/A3, is nearly identical for both sequences. Thus, the data suggest a normal Watson–Crick base pair involving this adenine in both duplexes, as depicted in Figure 1C (right).

NMR data were then acquired in D_2O to analyze the structures of both oligonucleotides by 2D methods. A comparison of the two duplexes via 150 ms mixing time NOESY experiments is shown in Figure S3; data for the methylated duplex alone are given in Figure 3. The data show that normal base stacking is present for both RNA duplexes, as confirmed by an intact tracing of the intra- and internucleotide

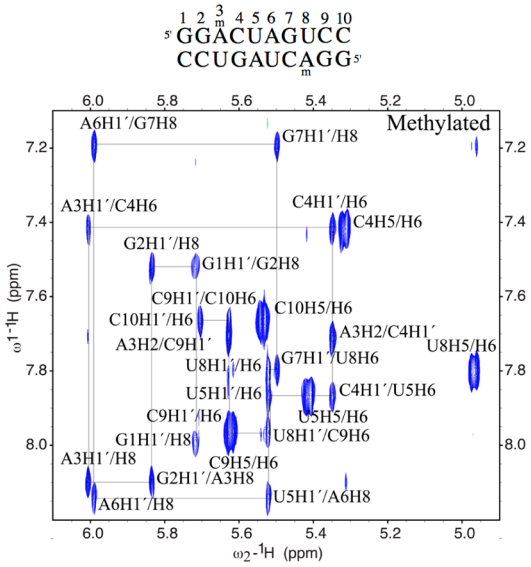

Figure 3. H1′/aromatic portion of a 150 ms mixing time NOESY in D_2O is shown for the methylated MA duplex, highlighting the sequential assignments of all bases. Sequence is 5′-GGACUAGUCC, where the bold base is methylated.

NOEs throughout the sequence. The similar NOE intensities for these data as well as other regions of the NOESY spectra (not shown) suggest that the structures of the two duplexes are similar, with 10 base pairs in each and sequential base stacking throughout. Slight chemical shift changes are observed for some resonances, chiefly on the base of *N*-methyladenosine, as well as the uridine that it is paired with, and adjacent nucleotides.

The *N*-methyl location and orientation were confidently assigned based upon NOESY data, which show clearly that the methylamino group is in the *anti* conformation. The NOEs observed in a 100 ms mixing time H_2O SS-NOESY experiment for the *N*-methyl resonance are highlighted in Figure S4. The observed NOEs fit with a group of protons on the Watson–Crick face of the base, as NOEs are observed to multiple NH and NH_2 resonances on the *N*-methyladenine base, the uridine that it is paired with, and the neighboring base pairs. Additionally, a weak NOE is observed to H8 of *N*-methyladenosine, confirming that the methyl group is rotated toward the H8 proton, and the NH of m^{6}A is rotated to hydrogen-bond with the U8-carbonyl.

The structural arrangement of the modified nucleobase and its methyl group are no doubt essential to its biophysical and biochemical properties. To further confirm the above structural assignment, we considered three possible base-pairing arrangements between the m^{6}A and uridine (Figure 1C). One of these (*syn*/*syn*) allows both two hydrogen-bonded base pairing and the favorable *syn* methyl orientation. However, the data clearly rule this out. Normal base stacking NOEs were observed from the sugar resonances of G2 and the sugar resonances of m^{6}A to the *N*-methyladenosine H8. If the base were in the *syn* conformation, then the H1′/H8 NOE would be very intense, but such a NOE is not observed. In addition, moderate intensity NOEs were observed to the H1′ of U4 and C9 from the *N*-methyladenosine H2, which are normal for an A-form helix. Furthermore, weak NOEs were observed at long mixing time from the methyl to the *N*-methyladenosine H8, as well as the G2 H8 and the C4 H5, which would not be observed if the methyl group were in the *syn* conformation. Further

DOI: 10.1021/ja513080v
J. Am. Chem. Soc. 2015, 137, 2107–2115

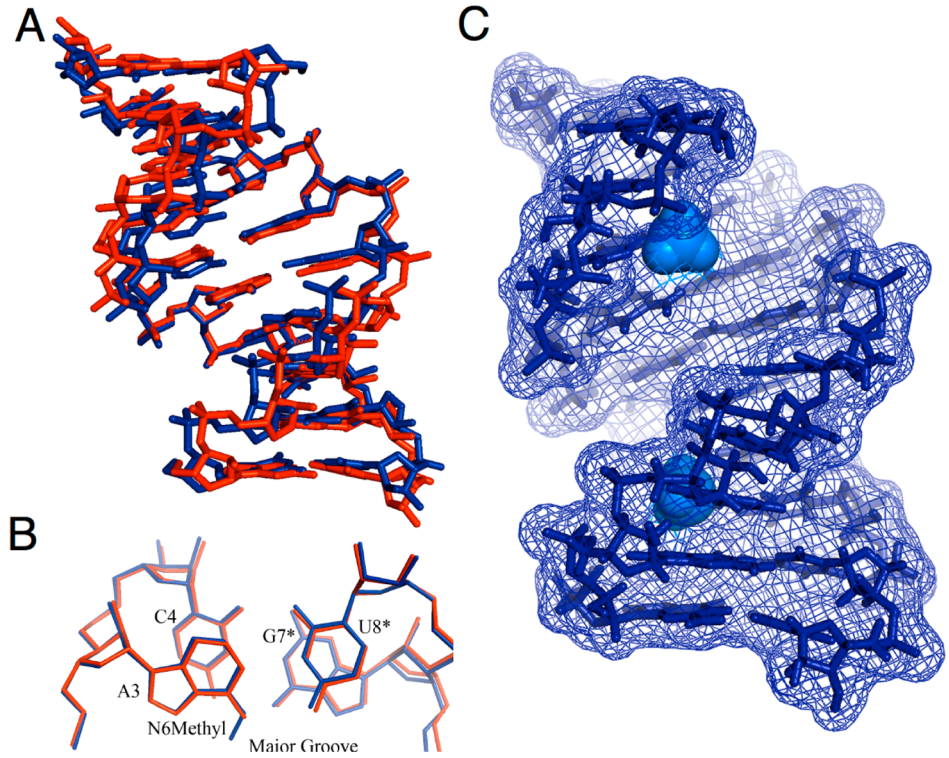

Figure 4. Structures of methylated and unmodified RNA duplexes, establishing that m^{6}A is oriented *anti* in a paired duplex, with the methyl group *anti* as well. (A) The average structure of the entire 10 bp duplexes with the MA in blue and unmodified DA RNA in red. (B) Superimposed structures of the second, third, and fourth base pairs alone; the m^{6}A3/U8*;A3/U8* and the neighboring base pair (C4/G7*) are shown for clarity. The second strands in the symmetric dimer are indicated with an asterisk (*). (C) Surface representation of the structure of the methylated RNA duplex, highlighting the adenine N6 methyl groups in the major groove (light blue).

confirmation that the assignments of H2 and the H8 of *N*-methyladenosine are not reversed is obtained from HSQC data, which confirms the H8 assignment at 8.1 ppm with a C8 shift of 137 ppm, in contrast to the H2 at 7.71 correlating to the C2 at 152 ppm.

In H_2O, intense NOEs were observed from the U8 imino to the *N*-methyladenosine H2 and NH but not the methyl group, also consistent with the methyl group rotated away from the U8 imino. Furthermore, the H2 rather than the H8 is close to the U8 imino proton, consistent with a Watson−Crick rather than a Hoogsteen base-pair. In addition, the NH of *N*-methyladenosine is sharp and shifted downfield to 8.34 ppm, suggesting two hydrogen bonds of a Watson−Crick A−U pair and ruling out the singly H-bonded (base *anti*/methyl *syn*) arrangement depicted in Figure 1C.

The amino portion of the 1D ^{1}H NMR in H_2O is shown in Figure S5. The NH of the N^6-methyladenosine is observed to be significantly sharper than the hydrogen-bonded amino resonance of the A3 in the unmodified duplex. This data suggests that rotation about the NH bond is slower for the *N*-methyl adenosine than for adenosine, leading to a sharper resonance. This is further highlighted in Figure S5B, showing the NOEs in the imino to amino/aromatic region in an SS-NOESY experiment. The NOE observed between the U8 imino and m^{6}A in the sequence is significantly more intense than that to the NH_2 of adenosine in the unmodified duplex. This data suggests that while the NH_2 of adenosine and the NH of N^6-methyladenosine are both hydrogen-bonded to U the slower rotation of the methylamino group results in a more intense NOE. Slower rotation about the C6−N6 bond in m^{6}A is no doubt the result of steric hindrance in the locally stacked and H-bonded base pairs, which would be temporarily disrupted by rotating the bulky methylamino group. Thus, local pairing traps the methylamino group in a high-energy conformation.

Solution structures were calculated for both oligonucleotide duplexes using 354 NOE derived distance constraints for the sequence with *N*-methyladenosine and 340 NOE derived distance constraints for the sequence with unmodified adenosine. Starting with 30 random structures, 25 converged to low energy for both molecules. A superposition of these 25 structures for each is shown in Figure S6. The overall heavy atom rmsd to the average structure was 0.87 Å for methylated RNA and 0.96 Å for the unmodified duplex.

A comparison of the average structure for each oligonucleotide is shown in Figure 4A. The rmsd between all heavy atoms of the two structures is 1.07 Å. The two structures are quite similar overall, with A-form helices containing 10 Watson−Crick base pairs. The only minor difference is a slight change in overall bending and winding of the helix, which is difficult to directly measure with only short-range NMR constraints. Superimposing only the six nucleotides of the second, third, and fourth base pairs, including the *N*-methyladenosine−uridine base pair and the two nucleotides above and below in the sequence, results in an rmsd of 0.22 Å. Thus, the local differences between the two structures are small. The m^{6}A methyl group is located in the major groove (Figures 4B,C and S7), with closest approach to N7 of the modified adenine and to major groove substituents on adjacent G and C bases in the GGACU consensus.

Nuclease Mapping of the Structures of Methylated Adenine Sites in Mammalian RNA. To determine the

DOI: 10.1021/ja513080v
J. Am. Chem. Soc. 2015, 137, 2107−2115

structural context and possible impact of m^{6}A in cellular RNAs, we compared the RNA secondary structure around methylated and nonmethylated adenosines in the RRACH motif. We recently determined the RNA secondary structure of the transcriptome of the human lymphoblastoid cell line GM12878 by parallel analysis of RNA structure (PARS).[20] To identify m^{6}A modification sites, we performed m^{6}A-IP-sequencing in GM12878 and also intersected our m^{6}A-enriched peaks with a high-resolution catalog of m^{6}A sites in diverse human cells.[28] For these high-confidence sites, we calculated the average PARS score for each nucleotide around m^{6}A-modified and unmodified RRACH motifs (Figure 5). The PARS score

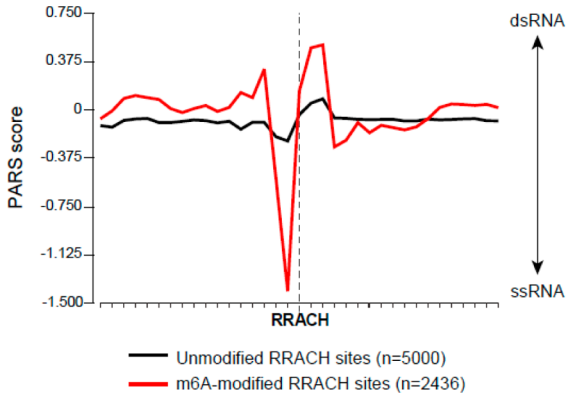

Figure 5. Nuclease structural mapping reveals a structural transition from unpaired to paired structure surrounding m^{6}A. Plot shows average PARS score for each nucleotide in the vicinity of methylated vs unmethylated adenines in the RRACH methylation consensus, as mapped for polyadenylated RNAs from GM12878 cells. Non-methylated sites were chosen as the 5000 sites with the lowest enrichment score after m^{6}A IP. *y*-axis represents PARS score. Positive values indicate high probability of double-stranded conformation, as evidenced by RNase V1 cleavage, whereas negative values indicate high probability of single-stranded conformation, as evidenced by RNase S1 cleavage. *x*-axis represents nucleotide position.

reflects the per base ratio of the number of reads obtained at cleavage sites by double- vs single-stranded nucleases and indicates whether a base is likely to be paired (positive score) or unpaired (negative score). We observed that methylated sites are clearly distinguished from unmodified sites through their structural profiles. In modified RNAs, there is a clear transition in average structure, as indicated by nuclease reactivity. In particular, the purine nucleotide immediately upstream of the modified A has a high probability of being single-stranded, with a strong negative PARS score. The methylated base itself has intermediate probability of being unpaired. In contrast, the two residues immediately to the 3′ side of m^{6}A show a significant tendency toward paired structure. Because the PARS data were generated from purified RNA refolded *in vitro*, the observed structural profile reflects information encoded in the RNA molecule itself, in the absence of influence from proteins such as m^{6}A readers.[15] These results with cellular mRNAs suggest that methylation occurs to situate the methyl group in between unpaired RNA and adjacent to helices, which our thermodynamic data suggest is the most energetically favorable outcome.

DISCUSSION

Taken together, our data show that the m^{6}A–U pair in a stable RNA duplex is paired in canonical configuration, with two Watson–Crick hydrogen bonds. To accommodate this, the N^6-methyl group in the modified duplex is rotated into the high-energy *anti* conformation, with the methyl group aimed directly into the major groove of the RNA, where the amino proton would normally be. This is further highlighted in the surface representation in Figure 4b, showing the methyl projecting into the groove. Closest contacts with the methyl group include the major groove edges of the bases above and below (G2 and C4, Figure S7).

Previous NMR studies of the m^{6}A nucleobase in free solution have shown that the methylamino group prefers the *syn* conformation, with an energetic preference of ca. 1.5 kcal/mol.[16] This preference is likely due to steric clashing of the methyl group with N7 in the *anti* arrangement. Thus, our experiments confirm that formation of an m^{6}A–U base pair requires flipping and trapping of the methylamino group into an energetically unfavorable spring-loaded orientation. This is partially compensated for by hydrogen bonding and Watson–Crick geometry matching with U (Figure 1C); the end result is the net destabilization of the duplex by 0.5–1.7 kcal/mol for a single methyl substitution. Studies of 6-methyldeoxyadenosine in duplex DNA suggest that the methyl group slows hybridization,[29] which is consistent with a requirement for rotation of the methylamino group into a high-energy conformation before base pairing can occur. Thus, we conclude that, when paired in RNA with stable base pairing surrounding it, m^{6}A acts as a compressed spring that is locked into place by its paired context.

Our finding of this Watson–Crick paired geometry helps to explain the enzymatic properties of m^{6}A. Most reverse transcriptase enzymes are able to read through this modification with little difficulty[19] and to pair it with T, as expected for the canonical paired geometry. This would not be expected if non-Watson–Crick orientations (Figure 1C) were found. Such reverse transcriptases may have sufficient steric room in the major groove to accommodate the *anti* methyl group with little penalty. However, at least one polymerase (*Tth*, a DNA polymerase that also exhibits reverse transcriptase activity) does show ca. 10-fold selectivity against the methyl modification,[19] which may reflect more sterically restrictive interactions with the major groove.

Our data help to clarify conflicting early studies that measured pairing effects of m^{6}A in the duplex context. While experiments by Kierzek with various adenine N-substitutions showed thermodynamic destabilization by methyl substitution,[25] a study by Micura of m^{6}A in a longer duplex context showed no destabilization by this modification.[30] Our data, measured with short duplexes, are consistent with Kiezek's measurements, and we hypothesize that a long duplex context masks the effects of single m^{6}A substitutions.

In contrast to this duplex destabilization, methylation of adenosine adjacent to helices is shown here to stabilize the overall structure substantially by enhancing base stacking, contributing 0.4–0.6 kcal of extra stabilization. m^{6}A in unpaired environments is known to adopt the relaxed (*syn*) conformation.[16,17] This would have the effect of placing the methyl group in contact with the adjacent base pair, which likely adds favorable hydrophobic stabilization.[27]

As a result of these opposing effects, we hypothesize that enzymatic methylation and demethylation could affect RNA conformations more globally. For example, methylation of adenine within a duplex region would destabilize it. If the local duplex surrounding the methylation site is not highly stable,

DOI: 10.1021/ja513080v
J. Am. Chem. Soc. 2015, 137, 2107–2115

then this could drive unwinding, leading to a less folded structure on average. Such a conformational effect was previously hypothesized by Micura,[30] although destabilization by m^{6}A was not observed in that study. Such unwinding could well have biological consequences: experiments have shown that elimination of duplex structures in RNAs can lead to more rapid degradation.[31,32] Similarly, genome-wide studies in yeast have shown a correlation of low melting temperatures with degradation by the exosome.[33] Thus, methylation in duplex regions could affect cellular lifetime of the RNA by making it more accessible to nucleases. In this light, it has been shown that methylated RNAs do, in fact, have a shorter cellular lifetime than unmethylated RNAs.[4] The preferential location of m^{6}A in 3′-UTRs is also consistent with this idea, given that duplex structure in 3′-UTRs is associated with increased lifetimes.[31]

We also speculate that such methylation of A in a duplex context could also lead, in principle, to a bimodal conformation switch to a second folded structure, which could be further stabilized by stacking if the m^{6}A residue is unpaired but near a helical region in the second structure. The newly emplaced m^{6}A residue in this scenario would act as a spring-loaded switch, driving local helix unpairing and resulting in the methylamino group flipping from *anti* to the more stable *syn* orientation. Once unpaired, the modified base could fold into a second conformation in which m^{6}A remains favorably unpaired and gains stacking interactions with neighboring helices. The overall driving force for a single methylation event of this type would be the combined energetic effects of *syn* preference and stacking, totaling from 0.9 to as much as 2.3 kcal/mol from the current data. Conversely, enzymatic demethylation of unpaired m^{6}A would have the opposite effect, decreasing beneficial stacking and favoring, relatively speaking, an RNA conformation in which the base is paired.

If such a switching mechanism were active, then we would expect it to be found in RNA contexts where two RNA folds were balanced reasonably closely in energy, although changes in methylation state at more than one site could magnify the energetic influence on conformations. If such switching occurs, then one would expect methylated adenine residues in such GGACH motifs to be preferentially located between unpaired bases and helices, having switched to that favorable conformation. Significantly, our PARS mapping data for methylated RNAs isolated from a human cell line do show striking evidence that m^{6}A is preferentially situated in such a structural context. Notably, we find a preference for 5′ location of m^{6}A next to helical structure, which is precisely the most stabilizing context for methylation in our thermodynamics studies (Table 2). Our thermodynamics data suggest that a dangling 3′ location of m^{6}A would also be favorable, although less so than 5′ stacked locations. Where the m^{6}A-stacked situation occurs in cellular RNAs, it appears to be dominated by the 5′ location in frequency, as judged by the PARS data. Whether this nuclease-mapped context is static or changes dynamically with methylation/demethylation remains to be seen; this hypothesis could be tested further by *in vivo* and *in vitro* structure probing[34] of methylated versus unmethylated RNAs.

Our data show that m^{6}A modification and context have substantial influences on RNA stability and structure. However, such effects may not be limited to RNA alone; for example, m^{6}A-binding proteins[4,35,36] may influence, and be influenced by, the dynamic conformation changes associated with the modification. A recent structural study of a YTH domain bound to an m^{6}A-containing RNA reveals m^{6}A in its relaxed *syn* conformation and present in a deep pocket.[36] This suggests that methylation of A in a double-stranded context would assist protein binding either by destabilizing the helix around it, thus allowing protein access, or by causing a conformation change to place m^{6}A in a single-stranded context. Thus, although our data show that methylation can affect RNA structure and stability without the aid of proteins, it is also quite possible that both may act together to affect RNA structure as well.

Also relevant to m^{6}A context are the structural preferences of methylating and demethylating enzymes. The structural preference of the METTL3 methylation complex for adenine methylation in the RRACH consensus is as yet unclear;[37] we would predict a preference for duplex contexts (prior to methylation) if methyl-driven unwinding or conformational switching is a widely active mechanism. Conversely, demethylating enzymes should exhibit a preference for unpaired m^{6}A in this scenario. Interestingly, the enzyme FTO, known to have m^{6}A demethylase activity, does appear in preliminary studies to prefer unpaired RNA as a context for demethylation over duplex structure,[7] which is consistent with our hypothesis. Future work will address these issues in detail.

■ ASSOCIATED CONTENT

Supporting Information

Additional experimental methods. Table S1: Mass spectrometry data for oligonucleotides. Figure S1: Representative thermal denaturation curves. Figure S2: Representative van't Hoff plots. Figure S3: The H1′/aromatic portion of NOESY data showing sequence connectivity. Figure S4: NOEs from the methyl group of *N*-methyl adenosine. Figure S5: Amino/imino NMR resonances and NOEs in water. Figure S6: Comparison of the superposition of 25 structures of each duplex. Figure S7: View of m^{6}A in the major groove of the methylated MA duplex. This material is available free of charge via the Internet at http://pubs.acs.org.

■ AUTHOR INFORMATION

Corresponding Authors

*(H.Y.C.) howchang@stanford.edu
*(E.T.K.) kool@stanford.edu

Notes

The authors declare no competing financial interest.

■ ACKNOWLEDGMENTS

We thank the U.S. National Institutes of Health (GM068122 and GM067201 to E.T.K.; R01-HG004361 and P50-HG007735 to H.Y.C.) for support. C.R. acknowledges the Swiss National Science Foundation for a postdoctoral fellowship.

■ REFERENCES

(1) Schibler, U.; Kelley, D. E.; Perry, R. P. *J. Mol. Biol.* **1977**, *115*, 695−714.
(2) Dominissini, D.; Moshitch-Moshkovitz, S.; Schwartz, S.; Salmon-Divon, M.; Ungar, L.; Osenberg, S.; Cesarkas, K.; Jacob-Hirsch, J.; Amariglio, N.; Kupiec, M.; Sorek, R.; Rechavi, G. *Nature* **2012**, *485*, 201−206.
(3) Meyer, K. D.; Saletore, Y.; Zumbo, P.; Elemento, O.; Mason, C. E.; Jaffrey, S. R. *Cell* **2012**, *150*, 1−12.

DOI: 10.1021/ja513080v
J. Am. Chem. Soc. 2015, 137, 2107−2115

(4) Wang, X.; Lu, Z.; Gomez, A.; Hon, G. C.; Yue, Y.; Han, D.; Fu, Y.; Parisien, M.; Dai, Q.; Jia, G.; Ren, B.; Pan, T.; He, C. *Nature* **2014**, *505*, 117−120.
(5) Csepany, T.; Lin, A.; Baldick, C. J., Jr.; Beemon, K. *J. Biol. Chem.* **1990**, *265*, 20117−20122.
(6) Bokar, J. A.; Shambaugh, M. E.; Polayes, D.; Matera, A. G.; Rottman, F. M. *RNA* **1997**, *3*, 1233−1247.
(7) Jia, G.; Fu, Y.; Zhao, X.; Dai, Q.; Zheng, G.; Yang, Y.; Yi, C.; Lindahl, T.; Pan, T.; Yang, Y. G.; He, C. *Nat. Chem. Biol.* **2011**, *7*, 885−887.
(8) Zheng, G.; Dahl, J. A.; Niu, Y.; Fedorcsak, P.; Huang, C. M.; Li, C. J.; Vågbø, C. B.; Shi, Y.; Wang, W. L.; Song, S. H.; Lu, Z.; Bosmans, R. P.; Dai, Q.; Hao, Y. J.; Yang, X.; Zhao, W. M.; Tong, W. M.; Wang, X. J.; Bogdan, F.; Furu, K.; Fu, Y.; Jia, G.; Zhao, X.; Liu, J.; Krokan, H. E.; Klungland, A.; Yang, Y. G.; He, C. *Mol. Cell* **2013**, *49*, 18−29.
(9) Gerken, T.; Girard, C. A.; Tung, Y. C.; Webby, C. J.; Saudek, V.; Hewitson, K. S.; Yeo, G. S.; McDonough, M. A.; Cunliffe, S.; McNeill, L. A.; Galvanovskis, J.; Rorsman, P.; Robins, P.; Prieur, X.; Coll, A. P.; Ma, M.; Jovanovic, Z.; Farooqi, I. S.; Sedgwick, B.; Barroso, I.; Lindahl, T.; Ponting, C. P.; Ashcroft, F. M.; O'Rahilly, S.; Schofield, C. J. *Science* **2007**, *318*, 1469−1472.
(10) Zheng, G.; Dahl, J. A.; Niu, Y.; Fu, Y.; Klungland, A.; Yang, Y. G.; He, C. *RNA Biol.* **2013**, *10*, 915−918.
(11) Kaklamani, V.; Yi, N.; Sadim, M.; Siziopikou, K.; Zhang, K.; Xu, Y.; Tofilon, S.; Agarwal, S.; Pasche, B.; Mantzoros, C. *BMC Med. Genet.* **2011**, *12*, 52−61.
(12) Garcia-Closas, M.; Couch, F. J.; Lindstrom, S.; Michailidou, K.; Schmidt, M. K.; Brook, M. N.; Orr, N.; Rhie, S. K.; Riboli, E.; Feigelson, H. S.; Le Marchand, L.; Buring, J. E.; Eccles, D.; Miron, P.; Fasching, P. A.; Brauch, H.; Chang-Claude, J.; Carpenter, J.; Godwin, A. K.; Nevanlinna, H.; Giles, G. G.; Cox, A.; Hopper, J. L.; Bolla, M. K.; Wang, Q.; Dennis, J.; Dicks, E.; Howat, W. J.; Schoof, N.; Bojesen, S. E.; Lambrechts, D.; Broeks, A.; Andrulis, I. L.; Guénel, P.; Burwinkel, B.; Sawyer, E. J.; Hollestelle, A.; Fletcher, O.; Winqvist, R.; Brenner, H.; Mannermaa, A.; Hamann, U.; Meindl, A.; Lindblom, A.; Zheng, W.; Devillee, P.; Goldberg, M. S.; Lubinski, J.; Kristensen, V.; Swerdlow, A.; Anton-Culver, H.; Dörk, T.; Muir, K.; Matsuo, K.; Wu, A. H.; Radice, P.; Teo, S. H.; Shu, X. O.; Blot, W.; Kang, D.; Hartman, M.; Sangrajrang, S.; Shen, C. Y.; Southey, M. C.; Park, D. J.; Hammet, F.; Stone, J.; Veer, L. J.; Rutgers, E. J.; Lophatananon, A.; Stewart-Brown, S.; Siriwanarangsan, P.; Peto, J.; Schrauder, M. G.; Ekici, A. B.; Beckmann, M. W.; Dos Santos Silva, I.; Johnson, N.; Warren, H.; Tomlinson, I.; Kerin, M. J.; Miller, N.; Marme, F.; Schneeweiss, A.; Sohn, C.; Truong, T.; Laurent-Puig, P.; Kerbrat, P.; Nordestgaard, B. G.; Nielsen, S. F.; Flyger, H.; Milne, R. L.; Perez, J. I.; Menéndez, P.; Müller, H.; Arndt, V.; Stegmaier, C.; Lichtner, P.; Lochmann, M.; Justenhoven, C.; Ko, Y. D.; Gene ENvironmental Interaction and breast CAncer (GENICA) Network; Muranen, T. A.; Aittomäki, K.; Blomqvist, C.; Greco, D.; Heikkinen, T.; Ito, H.; Iwata, H.; Yatabe, Y.; Antonenkova, N. N.; Margolin, S.; Kataja, V.; Kosma, V. M.; Hartikainen, J. M.; Balleine, R.; kConFab Investigators; Tseng, C. C.; Berg, D. V.; Stram, D. O.; Neven, P.; Dieudonné, A. S.; Leunen, K.; Rudolph, A.; Nickels, S.; Flesch-Janys, D.; Peterlongo, P.; Peissel, B.; Bernard, L.; Olson, J. E.; Wang, X.; Stevens, K.; Severi, G.; Baglietto, L.; McLean, C.; Coetzee, G. A.; Feng, Y.; Henderson, B. E.; Schumacher, F.; Bogdanova, N. V.; Labrèche, F.; Dumont, M.; Yip, C. H.; Taib, N. A.; Cheng, C. Y.; Shrubsole, M.; Long, J.; Pylkäs, K.; Jukkola-Vuorinen, A.; Kauppila, S.; Knight, J. A.; Glendon, G.; Mulligan, A. M.; Tollenaar, R. A.; Seynaeve, C. M.; Kriege, M.; Hooning, M. J.; van den Ouweland, A. M.; van Deurzen, C. H.; Lu, W.; Gao, Y. T.; Cai, H.; Balasubramanian, S. P.; Cross, S. S.; Reed, M. W.; Signorello, L.; Cai, Q.; Shah, M.; Miao, H.; Chan, C. W.; Chia, K. S.; Jakubowska, A.; Jaworska, K.; Durda, K.; Hsiung, C. N.; Wu, P. E.; Yu, J. C.; Ashworth, A.; Jones, M.; Tessier, D. C.; González-Neira, A.; Pita, G.; Alonso, M. R.; Vincent, D.; Bacot, F.; Ambrosone, C. B.; Bandera, E. V.; John, E. M.; Chen, G. K.; Hu, J. J.; Rodriguez-Gil, J. L.; Bernstein, L.; Press, M. F.; Ziegler, R. G.; Millikan, R. M.; Deming-Halverson, S. L.; Nyante, S.; Ingles, S. A.; Waisfisz, Q.; Tsimiklis, H.; Makalic, E.; Schmidt, D.; Bui, M.; Gibson, L.; Müller-Myhsok, B.; Schmutzler, R. K.; Hein, R.; Dahmen, N.; Beckmann, L.; Aaltonen, K.; Czene, K.; Irwanto, A.; Liu, J.; Turnbull, C.; Familial Breast Cancer Study (FBCS); Rahman, N.; Meijers-Heijboer, H.; Uitterlinden, A. G.; Rivadeneira, F.; Australian Breast Cancer Tissue Bank (ABCTB) Investigators; Olswold, C.; Slager, S.; Pilarski, R.; Ademuyiwa, F.; Konstantopoulou, I.; Martin, N. G.; Montgomery, G. W.; Slamon, D. J.; Rauh, C.; Lux, M. P.; Jud, S. M.; Bruning, T.; Weaver, J.; Sharma, P.; Pathak, H.; Tapper, W.; Gerty, S.; Durcan, L.; Trichopoulos, D.; Tumino, R.; Peeters, P. H.; Kaaks, R.; Campa, D.; Canzian, F.; Weiderpass, E.; Johansson, M.; Khaw, K. T.; Travis, R.; Clavel-Chapelon, F.; Kolonel, L. N.; Chen, C.; Beck, A.; Hankinson, S. E.; Berg, C. D.; Hoover, R. N.; Lissowska, J.; Figueroa, J. D.; Chasman, D. I.; Gaudet, M. M.; Diver, W. R.; Willett, W. C.; Hunter, D. J.; Simard, J.; Benitez, J.; Dunning, A. M.; Sherman, M. E.; Chenevix-Trench, G.; Chanock, S. J.; Hall, P.; Pharoah, P. D.; Vachon, C.; Easton, D. F.; Haiman, C. A.; Kraft, P. *Nat. Genet.* **2013**, *45*, 392−398.
(13) Delahanty, R. J.; Beeghly-Fadiel, A.; Xiang, Y. B.; Long, J.; Cai, Q.; Wen, W.; Xu, W. H.; Cai, H.; He, J.; Gao, Y. T.; Zheng, W.; Shu, X. O. *Am. J. Epidemiol.* **2011**, *174*, 1115−1126.
(14) Jia, G.; Fu, Y.; He, C. *Trends Genet.* **2013**, *29*, 108−115.
(15) Wang, X.; He, C. *RNA Biol.* **2014**, *11*, 669−672.
(16) Engel, J. D.; von Hippel, P. H. *Biochemistry* **1974**, *13*, 4143−4158.
(17) Sternglanz, H.; Bugg, C. E. *Science* **1973**, *182*, 833−834.
(18) Engel, J. D.; von Hippel, P. H. *J. Biol. Chem.* **1978**, *253*, 927−934.
(19) Harcourt, E. M.; Ehrenschwender, T.; Batista, P. J.; Chang, H. Y.; Kool, E. T. *J. Am. Chem. Soc.* **2013**, *135*, 19079−82.
(20) Wan, Y.; Qu, K.; Zhang, Q. C.; Flynn, R. A.; Manor, O.; Ouyang, Z.; Zhang, J.; Spitale, R. C.; Snyder, M. P.; Segal, E.; Chang, H. Y. *Nature* **2014**, *505*, 706−9.
(21) Batista, P. J.; Molinie, B.; Wang, J.; Qu, K.; Zhang, J.; Li, L.; Bouley, D. M.; Lujan, E.; Haddad, B.; Daneshvar, K.; Carter, A. C.; Flynn, R. A.; Zhou, C.; Lim, K.; Dedon, P.; Wernig, M.; Mullen, A. C.; Xing, Y.; Giallourakis, C. C.; Chang, H. Y. *Cell Stem Cell.* **2014**, *15*, 707−719.
(22) Xiao, R.; Moore, D. D. *Current Protocols in Molecular Biology*; John Wiley & Sons: New York, 2011; Unit 21.21.
(23) Levin, J. Z.; Yassour, M.; Adiconis, X.; Nusbaum, C.; Thompson, D. A.; Friedman, N.; Gnirke, A.; Regev, A. *Nat. Methods* **2010**, *7*, 709−715.
(24) Trapnell, C.; Pachter, L.; Salzberg, S. L. *Bioinformatics* **2009**, *25*, 1105−11.
(25) Kierzek, E.; Kierzek, R. *Nucleic Acids Res.* **2003**, *31*, 4472−4480.
(26) Petersheim, M.; Turner, D. H. *Biochemistry* **1983**, *22*, 256−263.
(27) Guckian, K. M.; Schweitzer, B. A.; Ren, R. X.-F.; Sheils, C. J.; Tahmassebi, D. T.; Kool, E. T. *J. Am. Chem. Soc.* **2000**, *122*, 2213−2222.
(28) Schwartz, S.; Mumbach, M. R.; Jovanovic, M.; Wang, T.; Maciag, K.; Bushkin, G. G.; Mertins, P.; Ter-Ovanesyan, D.; Habib, N.; Cacchiarelli, D.; Sanjana, N. E.; Freinkman, E.; Pacold, M. E.; Satija, R.; Mikkelsen, T. S.; Hacohen, N.; Zhang, F.; Carr, S. A.; Lander, E. S.; Regev, A. *Cell Rep.* **2014**, *8*, 284−296.
(29) Fazakerley, G. V.; Guy, A.; Téoule, R.; Quignard, E.; Guschlbauer, W. *Biochimie* **1985**, *67*, 819−822.
(30) Micura, R.; Pils, W.; Höbartner, C.; Grubmayr, K.; Ebert, M. O.; Jaun, B. *Nucleic Acids Res.* **2001**, *29*, 3997−4005.
(31) Blum, E.; Carpousis, A. J.; Higgins, C. F. *J. Biol. Chem.* **1999**, *274*, 4009−4016.
(32) Koval, A. P.; Gogolevskaya, I. K.; Tatosyan, K. A.; Kramerov, D. A. *PLoS One* **2012**, *7*, e44157.
(33) Wan, Y.; Qu, K.; Ouyang, Z.; Kertesz, M.; Li, J.; Tibshirani, R.; Makino, D. L.; Nutter, R. C.; Segal, E.; Chang, H. Y. *Mol. Cell* **2012**, *48*, 169−181.
(34) Spitale, R. C.; Crisalli, P.; Flynn, R. F.; Torre, E. A.; Kool, E. T.; Chang, H. Y. *Nat. Chem. Biol.* **2012**, *9*, 18−20.
(35) Meyer, K. D.; Jaffrey, S. R. *Nat. Rev. Mol. Cell Biol.* **2014**, *15*, 313−26.

DOI: 10.1021/ja513080v
J. Am. Chem. Soc. 2015, 137, 2107−2115

(36) Xu, C.; Wang, X.; Liu, K.; Roundtree, I. A.; Tempel, W.; Li, Y.; Lu, Z.; He, C.; Min, J. *Nat. Chem. Biol.* **2014**, *10*, 927−929.
(37) Liu, J.; Yue, Y.; Han, D.; Wang, X.; Fu, Y.; Zhang, L.; Jia, G.; Yu, M.; Lu, Z.; Deng, X.; Dai, Q.; Chen, W.; He, C. *Nat. Chem. Biol.* **2014**, *10*, 93−95.

DOI: 10.1021/ja513080v
J. Am. Chem. Soc. 2015, 137, 2107−2115